A Feasibility Study on Tribological Origins of Knee Acoustic Emissions

Sevda Gharehbaghi, *Graduate Student Member, IEEE*, Hyeon Ki Jeong, Mohsen Safaei, and Omer T. Inan, *Senior Member, IEEE*

Abstract*—*Objective: **Considering the knee as a fluid-lubricated system, articulating surfaces undergo different lubrication modes and generate joint acoustic emissions (JAEs). The goal of this study is to compare knee biomechanical signals against synchronously recorded joint sounds and assess the hypothesis that JAEs are attributed to tribological origins.** ***Methods:*** **JAE, electromyography, ground reaction force signals, and motion capture markers were synchronously recorded from ten healthy subjects while performing two-leg and one-leg squat exercises. The biomechanical signals were processed to calculate a tribological parameter, lubrication coefficient, and JAEs were divided into short windows and processed to extract 64-time-frequency features. The lubrication coefficients and JAE features of two-leg squats were used to label the windows and train a classifier that discriminates the knee lubrication modes only based on JAE features.** ***Results:*** **The classifier was used to predict the label of one-leg squat JAE windows and it achieved a high test-accuracy of 84%. The Pearson correlation coefficient between the estimated friction coefficient and predicted JAE scores was 0.83 $\pm$ 0.08. Furthermore, the lubrication coefficient threshold, separating two lubrication modes, decreased by half from two-leg to one-leg squats. This result was consistent with tribological changes in the knee load as it was inversely doubled in one-leg squats.** ***Significance:*** **This study supports the potential use of JAEs as a quantitative biomarker to extract tribological information. Since arthritis and similar disease impact the roughness of the joint cartilage, the use of JAEs could have broad implications for studying joint frictions and monitoring joint structural changes with wearable devices.**

***Index Terms*—Joint acoustic emissions, vibroarthrography, biotribology, unsupervised learning, wearable technologies.**

Manuscript received May 14, 2021; revised August 27, 2021; accepted November 6, 2021. Date of publication November 10, 2021; date of current version April 21, 2022. This work was supported in part by the National Science Foundation/National Institutes of Health Smart and Connected Health Program under Grant 1R01EB023808, and in part by NSF under Grant 1749677. *(Corresponding author: Sevda Gharehbaghi.)*

Sevda Gharehbaghi is with the School of Electrical and Computer Engineering, Georgia Institute of Technology, Atlanta, GA 30332 USA (e-mail: sevda@gatech.edu).

Hyeon Ki Jeong and Omer T. Inan are with the School of Electrical and Computer Engineering, Georgia Institute of Technology, USA.

Mohsen Safaei was with the School of Electrical and Computer Engineering, Georgia Institute of Technology, USA. He is now with the Huxley Medical Inc., USA.

Digital Object Identifier 10.1109/TBME.2021.3127030

I. Introduction

VIBROARTHROGRAPHIC (VAG) signals or joint acoustic emissions (JAEs) are referred to vibrations or sounds emitted during joint articulation [1]–[3]. These vibrations can be generated from various inter-joint compartments and thus are hypothesized to be associated with different roughness, softening, or lubrication state in articulating surfaces [4]–[6]. JAEs can be measured non-invasively during routinely performed exercises such as flexion/extension, squats, and sit-to-stand in the standard clinic examination or with wearable smart braces at home [7]–[11]. The knee is one of the most complex joints in the human body and it is a hinge type joint lubricated with synovial fluid, protected by articular cartilages [12]. Since knees have an important role in bearing the whole body weight, they are susceptible to injuries and early degeneration of articular surfaces [13]. Recent studies have shown that structural changes in the joint, such as meniscus and ligaments tears or cartilage degeneration in arthritis disease, lead to changes in JAEs compared to those of healthy joints [12], [14]–[17]. The impact of changes in mechanical loading on joint sounds were also investigated in [18], [19]. Particularly, a recent work demonstrated that JAEs can be used to estimate joint load [20]. Moreover, the friction forces and JAEs of human joints are qualitatively studied in [21].

Due to similarities between the synovial joints such as knee and hip to engineering bearings, the lubrication mechanism in these joints are often simplified and modeled as fluid-film lubrication [22]. The articulating film formed between knee compartments has a dynamic shape and thickness that changes during articulation [23]. As a result, knees may experience different lubrication modes at certain flexion phases and pressure levels, namely boundary lubrication (BL) and hydrodynamic lubrication (HL) [24]. During BL mode, there is almost a solid on solid contact where lubrication is mostly governed by chemical reactions and lubricant particles at the cartilage surfaces rather than viscous properties of synovial fluid, resulting in a higher friction coefficient. On the other hand, during HL mode, a lubrication film is formed between the articulating surfaces and a lower friction coefficient is achieved [22], [23]. Since the knee has a complex structure, a mixed lubrication mode can also exist at certain flexion phases where both HL and BL modes are present at different knee interfaces.

From the tribological standpoint, the friction coefficient variations in the entire range of lubrication can be shown on a Stribeck curve [25], [26]. For soft permeable surfaces (e.g., articular

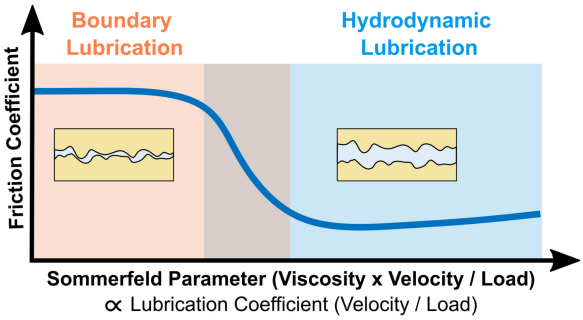

Fig. 1. Stribeck curve [25] and different lubrication modes. During boundary lubrication mode, there is a solid on solid contact, whereas during hydrodynamic lubrication, a lubrication film is formed between the articulating surfaces.

cartilages), the Stribeck curve is shown in Fig. 1 [27], and the *x*-axis represents *Sommerfeld parameter*, which is directly proportional to the sliding velocity, lubricant viscosity, and inversely proportional to the joint load. A low Sommerfeld parameter is associated with a high *friction coefficient* (*y*-axis) and vice versa.

Since the lubricant viscosity in the knee only experiences small changes in healthy joints [23], [28], and the information about rheological properties of the synovial fluid for each individual was not available for this study, we used a modified version of the Sommerfeld parameter. This parameter is called *lubrication coefficient*, and it is equal to the knee angular velocity divided by the knee joint load. This joint load or joint contact force (JCF) is the force experienced at knee articulating surfaces, and it cannot be measured directly through non-invasive methods; The current standard method for JCF estimation is through musculoskeletal modeling [20], [29].

The goal of this study is to explore the relationship between JAEs and the tribology of knee joint at different knee angles and two loading conditions. To the best of our knowledge, in this work, we established a quantified correlation between knee JAEs and lubrication coefficient for the first time, and that is evaluated for a normal activity such as squats. Demonstrating this quantified correlation shows that JAEs can include important information on knee tribology, which may help to establish a causal relationship between JAEs and degenerative diseases in vibroarthrography. The results of this study can help to improve the mechanistic understanding of the tribological origins of JAEs.

II. Materials and Methods

A. Demographics, Setup Description, and Data Collection

Ten healthy able-bodied subjects (10 male, age: 23 ± 2.9 years, height: 174.6 ± 4.9 cm, weight: 70.8 ± 10.4 kg) participated in this study under the approval from the Georgia Institute of Technology Institutional Review Board. Subjects with no history of major knee injury or surgery were able to participate in the study.

Each subject was instrumented with 20 reflective body motion capture markers to provide full 3D kinematics of the subject's lower limbs based on the Plug-In Gait lower body model [30].

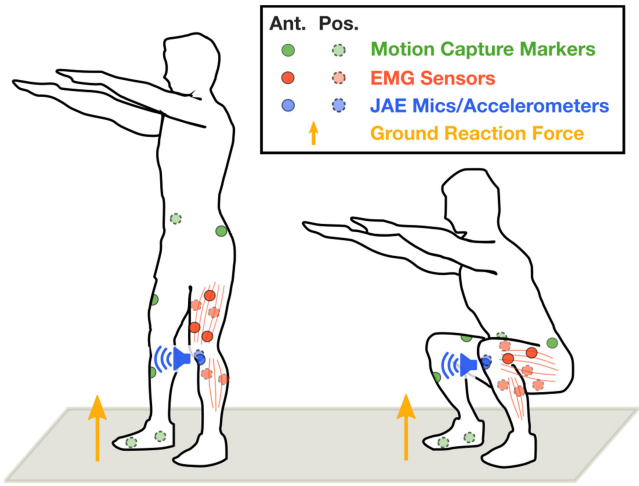

Fig. 2. Location of sensors in the experience setup.

Motion capture system at a sampling rate of 200 Hz (Vicon Motion Systems, Denver, CO, USA) was used to capture the motion trajectory. The ground reaction forces (GRF) and center of pressure on each leg was captured using a force plate (Bertec, Columbus, OH, USA) with a sampling rate of 1 kHz. Seven electromyography (EMG) sensors (Trigno Wireless EMG, Delsys, Natick, MA) were placed on key muscles targeted during squat exercises on the non-dominant leg (often left leg). These include rectus femoris, vastus lateralis, vastus medialis, biceps femoris, semitendinosus, and medial and lateral gastrocnemius [31]. The placement of these sensors is shown in Fig. 2.

Two miniature uniaxial accelerometers (series 3225, Dytran Instruments Inc., Chatsworth, CA, USA) were used to capture knee JAEs. They were attached to the medial and lateral sides of the patellar tendon on the left knee as these locations have been favored in previous studies for optimal contact area and mitigating the effect of soft tissue, muscle, and fat [15], [32]. A data acquisition system (NI USB-4432, National Instruments Corporation, Austin, TX) was used to capture these acoustic signals with a sampling rate of 25 kHz, and those were processed through MATLAB software (MathWorks, Natick, MA).

After being instrumented with these sensors, subjects were asked to perform 10 cycles of squats for two different conditions. The normal condition was defined as a two-leg squat with the foot stance of shoulder width, and the loaded condition was defined as a one-leg squat. The pace of the squat was controlled to be 4 seconds per cycle with a metronome to reduce the effect of speed on the acoustic emissions.

B. Inverse Dynamic Analysis

The motion capture trajectory data, GRF, and EMG signals were filtered and processed with the MATLAB MotoNMS toolbox [33]. OpenSim software was used to perform the standard inverse kinematics and inverse dynamics analyses and calculate JCF [34], [35]. A custom musculoskeletal model (MSKM) designed by Catelli *et al.* was used as this model allowed larger lower-limb range of motion for deep flexion exercises such as squats. [36]. The musculoskeletal model

was scaled to each subject's anthropometry based on the static trial. Muscle forces were computed using the Calibrated EMG-Informed Nueromusculoskeletal Modelling Toolbox (CEINMS) [37] which employs EMG-assisted algorithms to adjust excitation from the experimental EMG signals and synthesize rest that were not experimentally collected. JCF was then estimated using the muscle forces along with joint moments calculated from the joint reaction analysis. The resultant forces were segmented for each squat cycle and normalized to each subject's body weight (BW). The axial knee JCF and knee angular velocity were then used to compute the lubrication coefficient.

C. Preprocessing Joint Sounds and Feature Extraction

The recorded JAE signals from the contact microphones were divided into movement cycles ($\sim$ 4 seconds each) based on the kinematic markers. The high frequency noise was reduced by wavelet denoising with four levels of decomposition. The wavelet filter type was determined based on the minimum description length (MDL) criterion explained in [38]. Based on MDL criterion, we found that biorthogonal 6.8 (bior 6.8) wavelet filter requires the least number of coefficients to describe the JAE signals, which means that it best matches with the signals of this dataset. These JAEs carry high-energy and short-duration vibrations with "spike-like" waveforms which have a broad frequency spectrum mostly limited to 10 kHz [3], [39]. Thus, a Kaiser-window bandpass filter (250 Hz - 10 kHz) was used to further limit and reduce the unwanted noise and interference. After filtering, the recorded signals of each movement was divided into short-time, 50 ms, windows with an overlap of 80% between the successive windows. These heuristically chosen 50 ms JAE frames can be assumed as stationary signals [1] with only a few JAE signatures in them.

From these preprocessed windows, 64 audio features including temporal, spectral, Gammatone cepstral coefficients (GTCC) features were extracted. Temporal features consist of zero crossing rate (ZCR), energy, RMS amplitude, energy entropy, max-to-min, and five custom-designed distribution features (f_1 - f_{10}). Distribution features were defined based on the number of samples binned into the normalized ranges of [0 - 0.25 σ], [0 - 0.5 σ], [0 - 1 σ], [1 σ - 2 σ], and [2 σ - 3 σ]. Finally, Spectral features include spectral centroid, spectral crest, spectral decrease, spectral entropy, spectral flatness, spectral kurtosis, spectral roll-off, spectral skewness, spectral slope, spectral spread, harmonic ratios, fundamental frequency, mean frequency, 15 band power features (log-scaled frequency range between 250 Hz - 10 kHz), and 12 chroma features (f_{11} - f_{51}). The 13 GTCC features, modified from Mel-frequency cepstral coefficients (MFCC) features, use Gammatone (GT) filters in computing the spectral envelope shape which are adapted for non-speech audio classification purposes (f_{52} - f_{64}) [40]. All of these audio features except GTCCs and distribution have been used in previous works describing JAE signals [3], [15], [18], [19], [41].

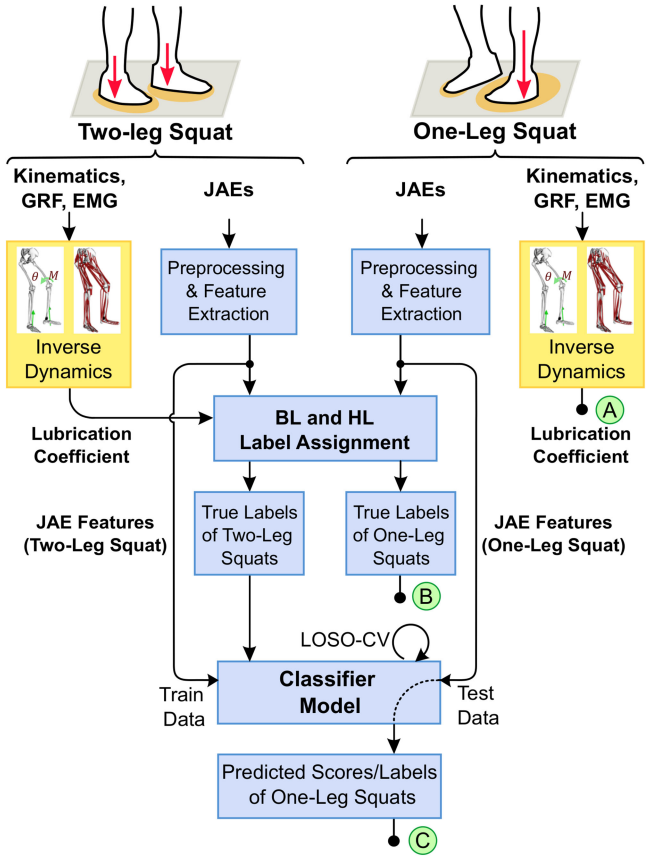

Fig. 3. Signal processing and machine learning pipeline. Kinematics, GRF, and EMG signals were processed with standard inverse dynamic analysis and lubrication coefficient was calculated separately for two-leg and one-leg squats. Besides, JAEs were preprocessed, windowed and features were extracted. The lubrication coefficients and JAE features of two-leg squats were used to assign BL/HL labels for both two-leg and one-leg windows and then train a classifier that discriminates the knee lubrication modes only based on JAE features. Then, the classifier was used to predict the label of one-leg squat JAE windows. The classifier performance was evaluated by comparing the true and predicted labels (points B and C). Also, the lubrication coefficients of one-leg squats was directly compared against the predicted joint sounds scores (points A and C).

D. Machine Learning

The goal of this step was to train a classifier that predicts the lubrication modes of knee frictions. Fig. 3 shows the signal processing and machine learning pipeline implemented in this study. After preprocessing and feature extraction of JAE signals, the feature matrix along with the synchronous lubrication coefficients were used to determine ground-truth labels of all joint sound events (1 for BL and 0 for HL). Then, a soft classifier was trained on two-leg squat events to estimate the probability of being attributed to the BL lubrication mode. A leave-one-subject-out cross-validation (LOSO-CV) loop was used for hyperparameter tuning and performance validation. Then, this trained classifier was used to predict the lubrication mode of one-leg squat events. The classifier performance can be evaluated by comparing the true labels and predicted labels of one-leg squat events (points B and C on the pipeline in Fig. 3).

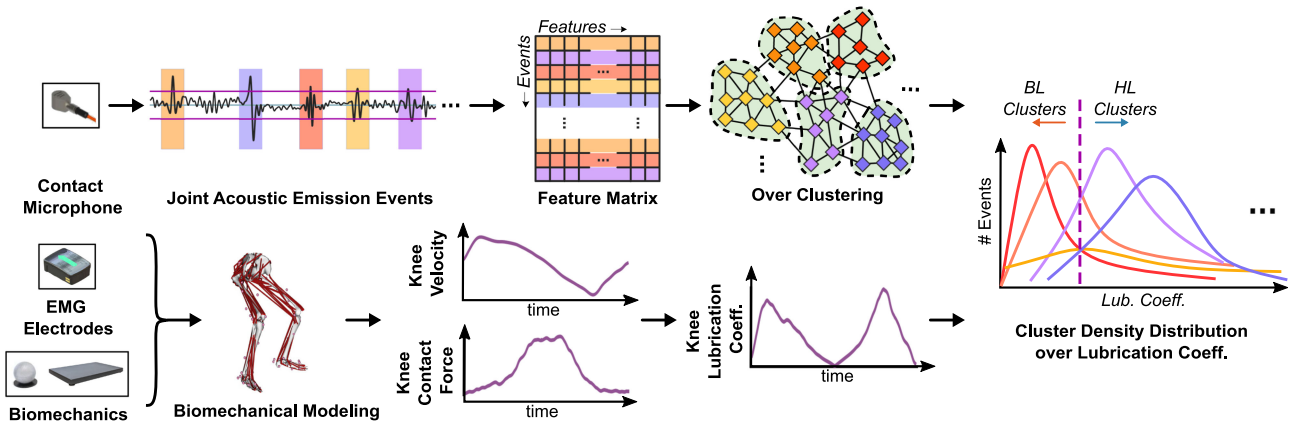

Fig. 4. Label assignment process. Over-clustering the JAE signatures based on the JAE features and determining the label of each group based on the associated lubrication coefficient distribution.

Note that the biomechanics data of only two-leg squats were used in the BL/HL label assignment, and the true labels of one-leg squat events were determined based on its similarity to two-leg squat events (i.e. the squared Euclidean distance in the feature space). To evaluate whether JAE events are attributed to the tribological origins, the lubrication coefficients of one-leg squats can be directly compared against the predicted joint sounds labels/scores (points A and C on the pipeline in Fig. 3). Note that the lubrication coefficients of one-leg squats were not used in the label assignment process and the classifier has never seen them. The results of this comparison are presented in Section III-D.

As a side note, we chose to use the two-leg squats data for classifier training because the total knee load in this case was determined based on body weight; whereas in one-leg squats, the subjects were asked to lean on the non-dominant leg while keeping the other leg on floor for balancing purposes. However, in practice, subjects tend to partially lean on both legs, which introduced uncertainties in the body weight distribution. For instance, some subjects had doubled the JCF in one-leg (compared to two-leg squat) by completely leaning on one leg, while others had the JCF increased by only 20%.

E. BL/HL Label Assignment

The synchronously recorded biomechanical data was used to determine the lubrication modes (BL/HL) of knee frictions. Based on Fig. 1, ideally, all events occurring at low lubrication coefficients should be labeled as BL, and those occurring at high values should be labeled as HL. In this ideal case, articulating surfaces would completely rub against each other during BL phase and glide easily with no direct surface contact at HL phase. If knee had a simple structure, the BL and HL events would have happened in distinct phases of the squat movement cycle. Thus, a simple threshold on the lubrication coefficient could potentially differentiate BL and HL events. However, the knee has a complex structure, and parts of articulating surfaces can be in close contact even at hydrodynamic lubrication phase [22]. In addition, the transition from one phase to the other one is gradual and continuous; Thus, BL and HL events may happen simultaneously at different parts of the knee in all the phases but with various density distributions. As a result, a simple threshold may poorly classify the BL and HL events.

We hypothesize that events with very similar signatures are likely to be generated from the same friction source, and the label assignment algorithm can be improved by accounting for the similarities between JAE events. So, instead of evaluating the label of each JAE event individually, we group JAE events with similar features and determine the label of each group separately. Intuitively speaking, we would like to calculate the median lubrication coefficient for each cluster and then label them based on a threshold. Fig. 4 illustrated this label assignment process where labels were determined based on both JAE features and associated lubrication coefficients.

1) Unsupervised Clustering of JAE Events: The JAE features of one-leg and two-leg squats were combined, having a total of about 85,000 JAE windows and 64 features. This combined dataset was divided into smaller groups of JAEs by over-clustering, so that each cluster could be assigned with the same BL/HL label. Since the recordings were windowed with a high overlap ratio of 80%, it is not expected to observe distinct clusters. Nevertheless, we would like to increase the number of clusters to make sure the events of each cluster includes very similar signatures. Therefore, the number of clusters was set to be higher than the optimal number of clusters determined by a density-based clustering algorithm. At the same time, if we divide the dataset into an unreasonably large number of clusters, the size of each cluster shrinks, and the output labels would approach to those of the individual event labeling output. This issue is further investigated in Appendix A.

2) Assigning Labels to Each Cluster: The label of each cluster was determined by comparing the lubrication coefficient distribution of JAE events in each cluster against a threshold. For instance, if most of the events in a cluster were happening at a low lubrication coefficient, the events of that cluster were all labeled as BL. This threshold can be set on the median (or a certain percentile) of the lubrication coefficients in each cluster.

Note that the JAE events of both one-leg and two-leg squats were divided into smaller clusters. However, only the lubrication

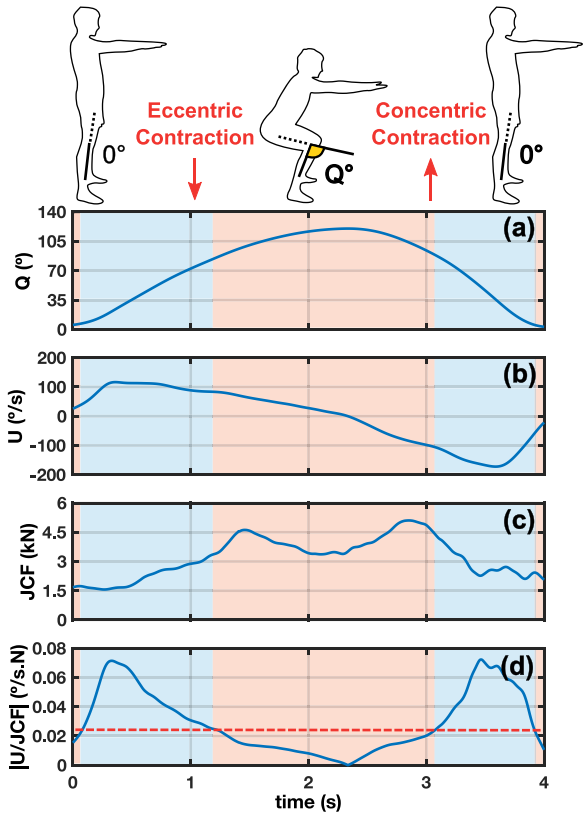

Fig. 5. Biomechanical parameters for a sample movement cycle. (a) Knee angle (Q) and (b) angular velocity (U) were collected based on the motion capture system. (c) Joint contact force (JCF) was estimated based on the inverse dynamic models. (d) Lubrication coefficient was calculated as the absolute ratio of angular velocity over JCF. Note that JCF maximized at full flexion (halfway in the cycle).

coefficients of two-leg squats were used to calculate the median value and compare that against a threshold. The JAE events of one-leg squats in each cluster were assigned with the same label as two-leg squat events of that cluster, which had similar feature sets.

III. Results and Discussion

A. Inverse Dynamic Analysis and Estimated Kinetics

Knee angle (Q °) and velocity (U °/s) were calculated through the synchronous knee kinematics captured from the motion markers. The knee flexion angle for the squat exercise has some inter-subject variability ranging from 0° in standing mode to up to about 140° in deep squat and back to 0° after a full squat cycle. Fig. 5(a) shows knee angle in a sample squat cycle. The knee angular velocity is the first derivation of the knee angle, increasing halfway in the eccentric contraction and decreasing to 0 (°/s) at full flexion. After a natural pause at deep squat, the angular velocity increases in the opposite direction and then decreases in absolute value till reaching zero again at full extension or standing mode. Although metronome was used to control the speed of the squatting, some subjects performed the exercise at slightly higher speeds. The angular velocity for all subjects were in a similar range and it varied between -200 °/s to +200 °/s. A sample knee angular velocity is shown in Fig. 5(b). JCF was estimated based on the standard inverse dynamic analysis and processing kinematics, GRF, and EMG signals. An estimated sample axial JCF (in N) is shown on Fig. 5(c). Note that although the average pace for each movement cycle is 4 seconds, the associated velocities with each 50 ms JAE is not the same (see Fig. 5(b)). As a result, two JAE windows with a similar joint loading but different velocities may belong to different lubrication modes (e.g., t = 2 sec and t= 3.2 sec in Fig. 5(c)) and the classifier should differentiate them. If this exercise is performed at a lower average speed, it will contribute to a lower Sommerfeld parameter, and it is expected to result in a wider BL phase.

The lubrication coefficient is computed by dividing the synchronous knee angular velocity to the estimated JCF, and the result is shown in Fig. 5(d). Since the JCF has a higher value around full flexion, the lubrication coefficient has a lower value in this phase. Similarly, the velocity was around zero at the starting and ending of the movement cycle as well as full flexion. Therefore, the lubrication coefficient is also very small at these phases. A threshold of ~ 0.03 is set on the lubrication coefficient in Fig. 5, and in an ideal case with distinct BL and HL lubrication phases, this threshold can separate the lubrication modes, presented with orange (BL) and blue (HL) shades. In reality, the density distributions of BL and HL modes overlap, but we expect to observe a similar trend with higher density of BL events around the full flexion and a higher density of HL events around the full extension.

To the best of our knowledge, the results from the CEINMS can be validated by comparing between experimental muscle excitations from EMG and muscle excitations calculated using the CEINMS and static optimization modes, and they indicate that output from CEINMS had both higher R2 and lower RMSE for each muscle.

B. Distribution of BL/HL Events Across Biomechanics

JAE events of two-leg and one-leg squats were over-clustered into 100 clusters with a k-means algorithm and based on the squared Euclidean distance in the feature space. The number of clusters was set to be greater than the optimal number (42 clusters) determined by DBSCAN clustering algorithm; this is further explained in Appendix A. The distribution of lubrication coefficients in each cluster was compared against a threshold to determine the label of that cluster. In this case, we labeled a cluster as BL mode when the median of the lubrication coefficients associated with two-leg squats were lower than a threshold of 0.03. This threshold value was set to maximize the separation of BL and HL lubrication coefficients, and it is investigated in more detail in Appendix B.

In this label assignment algorithm, we hypothesized that events with very similar JAE features are likely to be generated from the same source of friction. Thus, in the label assignment process, the similarity of JAE events were considered in addition to the biomechanical data. Now, it would be interesting to investigate how the BL/HL event distributions deviate from an ideal case with distinct lubrication phases. Fig. 6 (a, b) shows

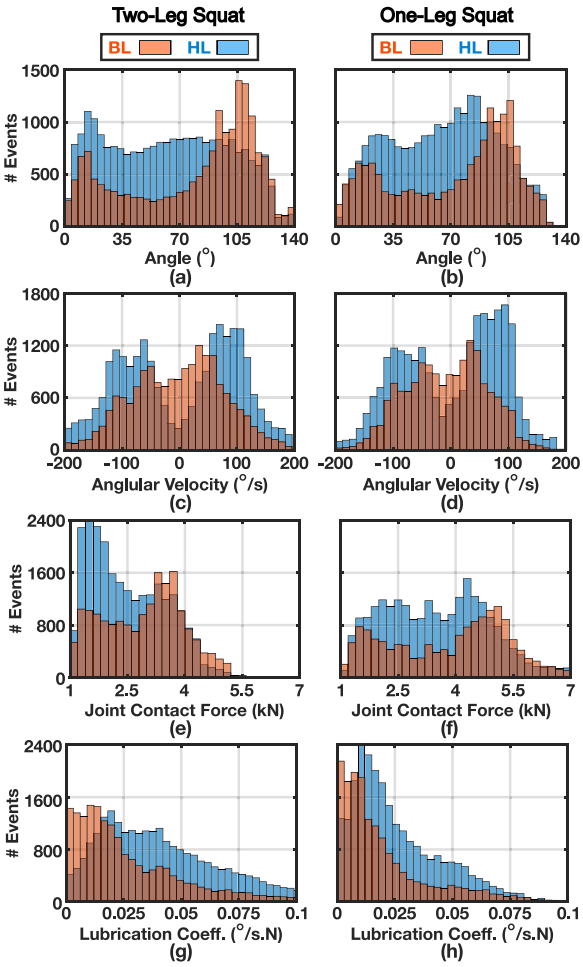

Fig. 6. Histograms of BL and HL events across biomechanical parameters: Knee flexion angle (a), (b); knee angular velocity (c), (d); axial Joint contact force (e), (f); and lubrication coefficient (g), (h) in two-leg squat and one-leg squat respectively.

the distribution of all the BL (in orange) and HL (in blue) events across the knee angle for two-leg and one-leg squats. The BL events were more frequent at full flexion, about 110° and 100° for two-leg and one-leg squats, respectively. This result was expected since in one-leg squats the non-dominant leg was bearing a higher body weight and thus the compressed articulating surfaces, under this extra loading condition, would reach to boundary lubrication at lower flexion angles. Density distributions of BL/HL events across angular velocity are demonstrates in Fig. 6 (c, d) for two-leg and one-leg squats. The BL events were dominantly occurring around the zero angular velocity, whereas the HL events have a bimodal distributions. Having two peaks for HL events was expected because of the symmetric motion in the eccentric and concentric contractions. The peak in positive velocities is associated with eccentric contraction and the negative peak represents the concentric contraction (also shown in Fig. 5). It's noteworthy that both BL and HL events have higher densities (higher peak) at eccentric contraction. This might be because the subjects tend to perform eccentric contraction slower than concentric contraction [42], and therefore in eccentric contraction joint sound events had a higher density. The BL and HL event distributions were significantly distinct ($p < 0.001$) in both two-leg squats and in one-leg squats. BL events have two peaks around $\pm 50°/s$, and HL events had peaks around $\pm 100°/s$, which also supports the distinct lubrication modes shown in Fig. 5.

Density distributions across JCF in two-leg and one-leg squats were shown in Fig. 6 (e, f). In two-leg squats, BL events occur more frequently at higher joint contact forces, while HL events occur at lower forces. However, in one-leg squat, those events are distributed over a wider range. This can be due to the high variability in one-leg loading conditions. The lubrication coefficient was calculated by dividing the angular velocity to the JCF, and it is demonstrated in Fig. 6 (g, h). It can be seen that as JCF was increased in one-leg compared to two-leg squats, and consequently the distribution of lubrication coefficients was shifted toward lower values. The lubrication coefficient threshold (the crossover point of BL and HL distributions) of one-leg squats was half of this parameter for two-leg squats. This change in lubrication coefficient threshold is consistent with our expectation since the median of JCF in one-leg squats is approximately twice that of two-leg squats.

C. Classification Performance

JAE events with similar features fell into the same clusters and got the same labels. To verify this, a classifier was trained with two-leg squat events and tested on one-leg squat events. With a basic classifier, logistic regression, a high CV accuracy of 86% and a test accuracy of 84% were achieved. Similarly, with a more advanced ensemble learning method, random forest, a CV accuracy of 89% and a test accuracy of 84% were achieved. The high test accuracy of both models confirms that a machine learning model could learn and distinguish BL vs. HL events properly. In other words, a classifier is also able to distinguish the JAEs based on their similarities and differences (the same way that clustering does). The kernel density distributions of some of the top features – namely GTCC, band power, MFCC, ZCR, harmonic ratio, and spectral centroid – are illustrated in Fig. 7. The distinct distribution of BL and HL events across the spectral centroid shows that most of the BL events have higher frequency content compared to HL events. This result is consistent with the studies conducted on friction induced vibrations in lubricating mechanical components [43], reporting that the frequency of vibrations generated during boundary friction is higher than the frequency of vibrations generated in hydrodynamic mode.

D. Correlation Between Joint Sounds and Tribology

To investigate the relationship between joint sounds and knee tribology, the distribution of BL and HL lubrication coefficients at two loading conditions were compared. For two-leg squats, the BL and HL labels were predicted during the cross-validation process, and for one-leg squats, the BL and HL labels were predicted by the trained classifier.

The density of lubrication coefficient for BL and HL events were plotted in Fig. 8(a) and (b) for two-leg and one-leg squat exercises, respectively. It can be seen that, at low lubrication coefficients (<0.01), the density of BL events was almost three

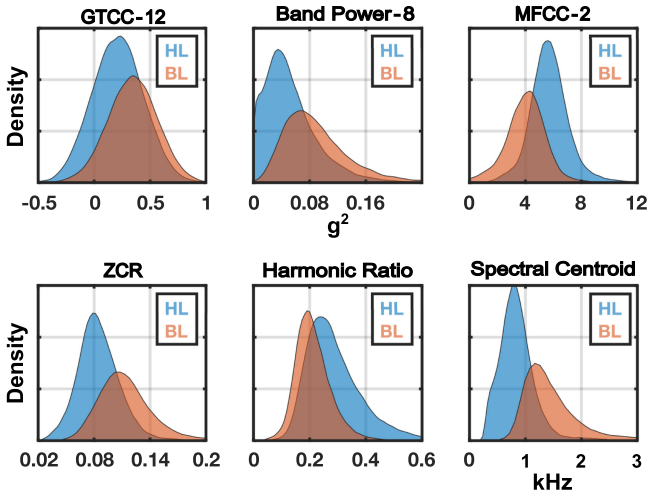

Fig. 7. Distinction of density distributions for BL and HL events in some of the top features.

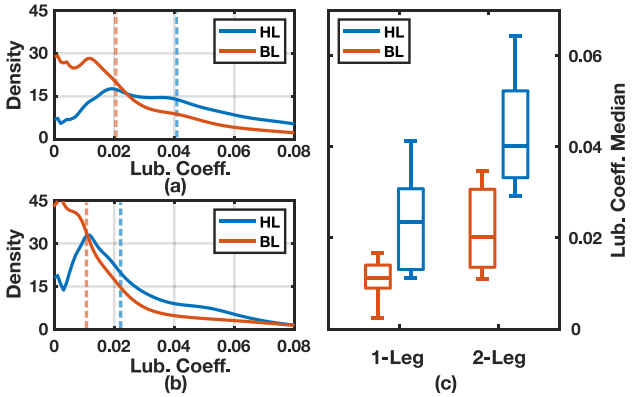

Fig. 8. Lubrication coefficient threshold shift from two-leg to one-leg: (a) kernel density distribution of two-leg squat events, (b) kernel density of one-leg squat events, (c) boxplots of lubrication coefficients median for each subject.

times higher than those of HL events, and at high lubrication coefficients (>0.04 in this study), the density of HL events was significantly higher than those of BL events. A study in [44] reports that articulating surfaces with velocities higher than 1 mm/s are operating in mixed lubrication mode. This means that the kernel density distributions of BL and HL events would overlap and this is consistent with our observation. The vertical lines in Figs. 8(a-b) show the median of the lubrication coefficients for BL and HL events, and Fig. 8(c) summarizes the statistics of these distributions for both datasets. Comparing the boxplots of one-leg and two-leg squats, the median of lubrication coefficient for BL events shifts down from 0.021 to about 0.011 which is consistent with our expectation, because the body load on the knee is almost doubled in one-leg squat exercise. To reiterate the similarity between joint sounds and biomechanical data, note that Figs. 8 (a, b) are similar to Figs. 6 (g, h), with a difference that in Fig. 6, BL and HL labels are assigned directly from biomechanical data, whereas in Fig. 8(b), the BL and HL groups were labeled via predictions from the classifier which distinguished them based on audio features.

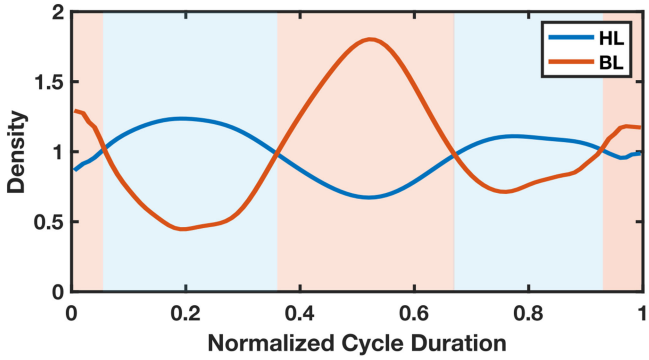

Fig. 9. Density distribution of BL and HL events calculated from the predicted labels of test dataset across normalized cycle duration.

The location of BL and HL phases calculated from lubrication coefficients of two-leg squats were compared against the distributions of BL and HL modes calculated from the predicted JAE labels of one-leg squats to provide more information about the relationship between joint sounds and knee tribology. Fig. 5(d) demonstrated the BL and HL phases for two-leg squats, and Fig. 9 illustrates the probabilities of occurring BL and HL JAE events in one-leg squats. Both figures present similar results where the probabilities of occurring BL events at the beginning, at the center, and at the end of the cycle, were higher than HL events, showing the potential use of joint sounds in determining the tribological phases.

In the next step, the JAEs and biomechanics data of one-leg squats were compared in a quantitative manner. The first row of Fig. 10 shows the estimated friction coefficient as a function of cycle duration for each subject. In these plots, the friction coefficients were estimated based on the lubrication coefficient, and the Stribeck curve was approximated with a sigmoid function (see Fig. 1). The second row of Fig. 10 shows the probability of BL phase, estimated by the logistic regression classifier, after applying a moving median filter. The dark blue trace shows the average value and the shaded area shows the standard deviation of the desired parameters across squat movement cycles.

Based on these plots, the friction coefficient (first row) and the BL scores (second row) were more or less consistent for each subject. We clearly see a peak in the friction coefficient/BL score around the center and sometimes at the beginning and ending of the movement cycle. The cross-correlation between these two parameters was calculated for each subject, and a high Pearson correlation coefficient of 0.83 ± 0.08 was achieved. It is expected to observe some differences in the first row and the second row, because the shape of the BL scores significantly depends on the subject's knee structure, which is not captured in the simplified estimation of the friction coefficient. Overall, Figs. 8–10 show various comparisons between the information extracted from joint sounds and those from biomechanical data. All of these comparisons represent that JAEs contain salient information on knee tribology.

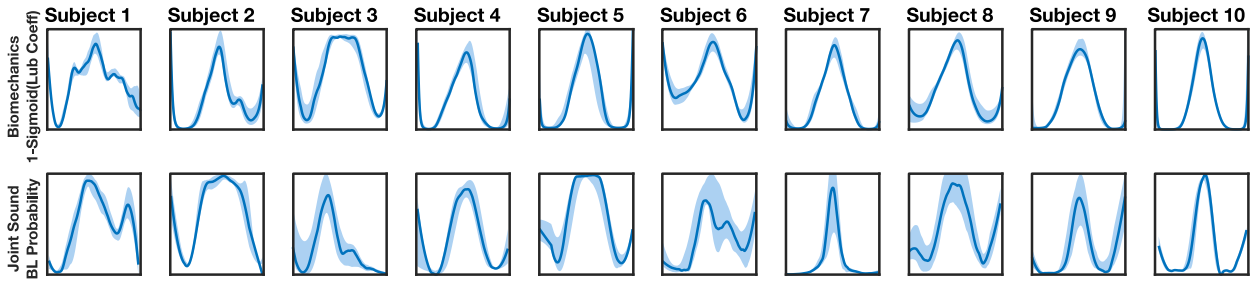

Fig. 10. Comparing the friction coefficient from one-leg squats biomechanical data (estimated from lubrication coefficients) for all the subjects in the first row, and the predicted probability of BL events for the same subjects in the second row. The cross-correlation between these two parameters was calculated for each subject, and a high Pearson correlation coefficient of 0.83 ± 0.08 was achieved.

IV. Significance and Limitations

The immediate goal of this preliminary study is to quantify the relationship between the tribological properties of the synovial joint and JAEs, which may help to establish a causal relationship between JAEs and degenerative diseases in vibroarthrography. In previous studies, JAEs were used as a digital biomarker in clinical applications to differentiate between healthy controls and subjects with degenerative diseases [1], [15], [19], [39]. Demonstrating a quantified correlation between JAEs and knee biomechanical parameters shows that JAEs can provide valuable physiological and pathological information about the joint which was previously only possible through measurements with multiple biomechanical sensors and estimations based on musculoskeletal models. In contrast with complex biomechanical measurement setups, this modality (i.e., JAEs) can be measured with wearable technologies for ambulatory applications and used as an assistive device to monitor patients' health in the clinic or at home.

No prior or independent information is available on the differences in knee joint structures that lead to vibrations [45]. Because of the lack of mechanistic understanding of JAEs, empirical techniques have been used to derive information from these signals. To understand the origins and characteristics of JAEs, the present work lays the groundwork that JAEs contain salient information on knee tribology in healthy subjects, while further studies on subjects with musculoskeletal injuries or arthritis are required. In such a study, the variations of the viscosity of the synovial fluid in affected knees should be considered [46], and MRI images could also provide valuable information about the knee structure. Investigating the effects of different injuries/diseases on knee structures and how that affects JAEs can help us develop algorithms to use JAEs as a biomarker to titrate care in patients.

The trained machine learning model in this work relies on the simulated JCF as a "ground truth" to calculate the lubrication coefficient, while this JCF is not directly measured in lab. Therefore, the accuracy of the ML model is limited to the accuracy of musculoskeletal simulations. Nonetheless, these simulations are one of the best methods for estimating in-vivo joint loads in healthy, able-bodied subjects [20] and current models are able to track joint load variations with R^2 of 0.91 and 0.7 for medial and lateral forces, respectively [47], which is promising when the relative changes in the joint forces are studied at different joint movement stages. Furthermore, there is an ongoing research to improve the musculoskeletal models and better estimate JCF.

In practice, JAEs are prone to be contaminated by artifacts such as loose microphone contacts, motion artifacts, hitting around microphone/wires, and setup issues. Some of these artifacts were identified in our previous works, and hardware modifications as well as signal processing steps were proposed to detect and improve the robustness of these algorithms [9], [16], [17], [19].

V. Conclusion and Future Work

In this work, we studied the acoustic emissions generated at different knee angles and loading conditions, and demonstrated for the first time that joint sounds are strongly correlated with knee tribology. These acoustic emissions contain salient information on knee tribology and they are able to predict the joint lubrication modes. One area of future work could be investigating the relationship between JAEs and biomechanics of both healthy and unhealthy knees with degraded cartilage surfaces and imbalanced force distribution happening in some disease or injuries. Because distinguishing the impact of structural changes in the JAEs depends on the richness of the input dataset that is fed into the ML model. It is expected to observe a higher rate of boundary lubrication induced acoustic events in degraded knees compared to healthy ones. This concept can also be investigated in a larger population and during other activities to improve our understanding and to achieve a more accurate quantified threshold for BL/HL classification. Lastly, finite element analysis can be coupled with inverse dynamic study to incorporate pressure distribution rather than JCF as a more precise representation of loading within the joint since contact movement patterns during articulation can change the force distribution on the joint interfaces.

Appendix A
Number of Clusters

In the label assignment algorithm, JAE events with similar features were grouped together, and a label was assigned to each

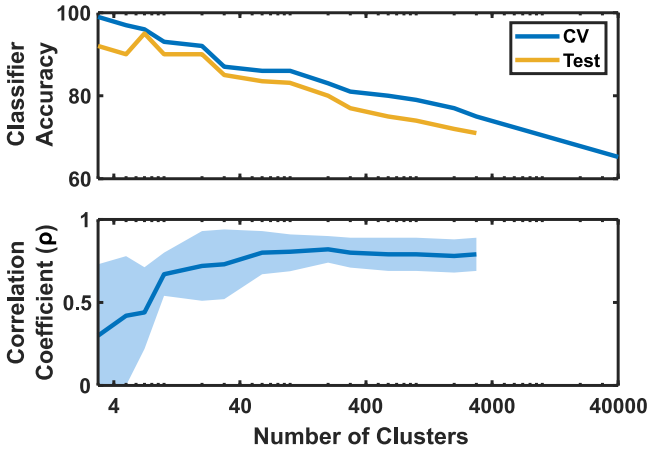

Fig. 11. Classifier performance and correlation coefficient between BL score and estimated friction coefficient as a function of number of clusters.

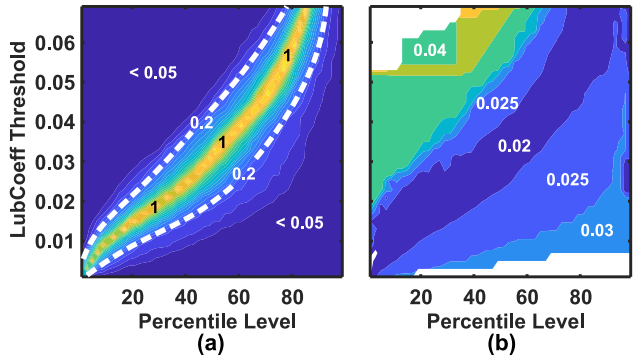

Fig. 12. (a) Dataset imbalance ratio and (b) distance between the median of lubrication coefficients of BL and HL groups in two-leg squats as a function of the two labeling hyperparameters.

group based on the associated lubrication coefficient distribution. Choosing the right number of clusters for label assignment affects the performance of the machine learning classifier and of course the labels of JAE events.

Assume a feature space representing these JAE events. If the dataset is divided into a small number of clusters, and each cluster was assigned to the same label, there would be a simpler decision boundary in the feature space that the classifier can learn and achieve a high accuracy. However, in this case, a diverse set of JAE events would be assigned to the same label, which would not be accurate. On the other hand, dividing the dataset into a large number of clusters ensures that JAE events in each cluster are more homogeneous, and the BL/HL label assignment based on the lubrication coefficient distribution would be more accurate. But the decision boundaries could be more complex and the classifier performance may degrade.

A density-based clustering algorithm was used to determine the optimal number of clusters. DBSCAN algorithm divided the dataset into 42 clusters, and we used 100 clusters to make the JAE signatures in each cluster more homogeneous. Fig. 11 shows the classifier validation and test accuracies and the Pearson correlation coefficient between BL scores and friction coefficients as a function of number of clusters. As the number of clusters increase and the decision boundary gets more complicated, the classifier encounters a more difficult learning task, and the accuracies decrease. In contrast, the correlation coefficient between BL score and friction coefficient increases with larger number of cluster, which may represent a better labeling performance, and then it plateaus for more than 42 clusters.

The two-leg squats dataset contains about 42000 JAE events. If each event was labeled individually, based on a lubrication coefficient threshold, that is the same as dividing the dataset into 42000 clusters. In this case, the cross-validation accuracy was 65%, and it follows the decreasing classifier accuracy trend.

In summary, the number of clusters should be higher than the optimal number of clusters determined by a hierarchical or density-based clustering algorithm to make sure the JAE events in each cluster are of the same type.

Appendix B
Label Assignment Hyperparameters

The label of each cluster was determined by comparing the lubrication coefficient distribution of JAE events in each cluster against a threshold. This threshold could be set on the median (or a certain percentile) of the lubrication coefficients of each cluster (see Fig. 4). The main criteria for selecting this threshold and percentile level is to improve the distinction between the density distributions of BL and HL groups. To be more specific, the difference between the median of BL and HL lubrication coefficients in Fig. 6(g) should be maximized. In addition, the size of one group should not be much bigger than the other group to facilitate the classifier learning.

Fig. 12(a) presents the dataset imbalance ratio, defined as the ratio of the minority class sample size to majority class sample size, across a 2D sweep of lubrication coefficient threshold and percentile level. The yellow diagonal curve indicates the trajectory that the dataset is balanced with equal number of samples in both classes. The two dashed lines also highlight the trajectories that one class is five times larger than the other class. Ideally, these two hyperparameters should be chosen from the area specified between the two dashed lines. Fig. 12(b) presents the distance between the median of BL and HL lubrication coefficient distributions across the 2D hyperparameter sweep. This distance does not change substantially as long as the hyperparameters are chosen inside the two dashed lines of Fig. 12(a). But for the hyperparameters outside this region, the size of one dataset is much larger than the other one (20:1 or more). In this case the distance between BL and HL groups may further increase. However, that is because the algorithm assigns all JAE events to one group except a few rare types of JAEs to the other group, which might not be insightful for this analysis.

The yellow diagonal trajectory on Fig. 12(a) shows hyperparameter combinations for having a balanced dataset. In addition, the distance between BL and HL groups on this trajectory does not change substantially. The classifier performance and the correlation coefficient between BL scores and the estimated

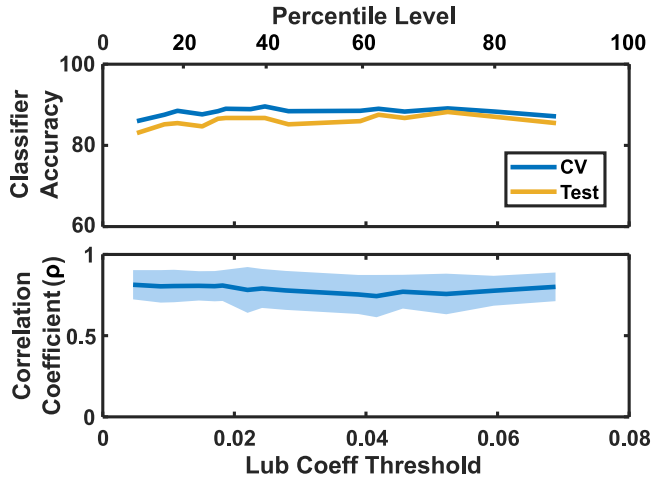

Fig. 13. Classifier performance and correlation coefficient between BL scores and estimated friction coefficients as a function of hyperparameter values.

friction coefficients are investigated for different choices of hyperparemeters on this trajectory, and the results are presented in Fig. 13. The lubrication coefficient thresholds and associated percentile levels are presented on the bottom and top x-axes. The classifier validation and test accuracies are almost constant. Also, the correlation coefficient does not change with the choice of hyperparameters. To give a numerical example, a label assignment criteria of "having 30% of the events with lubrication coefficients of higher than 0.02" is similar to the criteria of "having 50% of the events with lubrication coefficients of higher than 0.03". Fig. 13 confirms the strong correlation between JAE and knee tribology, independent from the exact choice of hyperparameters.

It is worth mentioning that choosing other combinations of hyperparameters might result in a degraded classifier performance or a smaller correlation coefficient; however, it does not undermine the earlier results shown in this study. Because the main goal was to show JAEs contain salient information on knee tribology, and that was demonstrated through the comparisons presented in the paper.

References

[1] S. Krishnan *et al.*, "Adaptive time-frequency analysis of knee joint vibroarthrographic signals for noninvasive screening of articular cartilage pathology," *IEEE Trans. Biomed. Eng.*, vol. 47, no. 6, pp. 773–783, Jun. 2000.

[2] S. Shrivastava and R. Prakash, "Assessment of bone condition by acoustic emission technique: A review," *J. Biomed. Sci. Eng.*, vol. 2, no. 3, 2009, Art. no. 144.

[3] S. Hersek *et al.*, "Acoustical emission analysis by unsupervised graph mining: A novel biomarker of knee health status," *IEEE Trans. Biomed. Eng.*, vol. 65, no. 6, pp. 1291–1300, Jun. 2018.

[4] R. M. Rangayyan *et al.*, "Parametric representation and screening of knee joint vibroarthrographic signals," *IEEE Trans. Biomed. Eng.*, vol. 44, no. 11, pp. 1068–1074, Nov. 1997.

[5] S. J. Song *et al.*, "Noise around the Knee," *Clin. Orthop. Surg.*, vol. 10, no. 1, pp. 1–8, 2018.

[6] D. C. Whittingslow *et al.*, "Acoustic emissions as a non-invasive biomarker of the structural health of the knee," *Ann. Biomed. Eng.*, vol. 48, no. 1, pp. 225–235, 2020.

[7] C. N. Teague *et al.*, "A wearable, multimodal sensing system to monitor knee joint health," *IEEE Sensors J.*, vol. 20, no. 18, pp. 10323–10334, Sep. 2020.

[8] D. M. Hochman *et al.*, "A pilot study to assess the reliability of sensing joint acoustic emissions of the wrist," *Sensors*, vol. 20, no. 15, 2020, Art. no. 4240.

[9] N. Bolus *et al.*, "Fit to burst: Toward noninvasive estimation of achilles tendon load using burst vibrations," *IEEE Trans. Biomed. Eng.*, vol. 68, no. 2, pp. 470–481, Feb. 2021.

[10] R. E. Andersen *et al.*, "A review of engineering aspects of vibroarthography of the knee joint," *Critical Rev. Phys. Rehabil. Med.*, vol. 28, pp. 1–2, 2016.

[11] H. Töreyin *et al.*, "Quantifying the consistency of wearable knee acoustical emission measurements during complex motions," *IEEE J. Biomed. Health Inform.*, vol. 20, no. 5, pp. 1265–1272, Sep. 2016.

[12] R. M. Rangayyan and Y. Wu, "Screening of knee-joint vibroarthrographic signals using statistical parameters and radial basis functions," *Med. Biol. Eng. Comput.*, vol. 46, no. 3, pp. 223–232, 2008.

[13] E. Ołowiana *et al.*, "Vibroarthrographic analysis of patellofemoral joint arthrokinematics during squats with increasing external loads," *BMC Sports Sci., Med. Rehabil.*, vol. 12, no. 1, pp. 1–9, 2020.

[14] Y. Wu, *Knee Joint Vibroarthrographic Signal Processing and Analysis*. Berlin, Germany: Springer, 2015, pp. 1–16.

[15] D. C. Whittingslow *et al.*, "Knee acoustic emissions as a digital biomarker of disease status in juvenile idiopathic arthritis," *Front. Digit. Health*, vol. 2, pp. 1–12, 2020.

[16] G. Ozmen *et al.*, "Detection of meniscal tear effects on tibial vibration using passive knee sound measurements," *IEEE Trans. Biomed. Eng.*, vol. 68, no. 7, pp. 2241–2250, Jul. 2021.

[17] K. L. Richardson *et al.*, "Quantifying signal quality for joint acoustic emissions using graph-based spectral embedding," *IEEE Sensors J.*, vol. 21, no. 12, pp. 13 676–13 684, Jun. 2021.

[18] H. K. Jeong *et al.*, "Quantifying the effects of increasing mechanical stress on knee acoustical emissions using unsupervised graph mining," *IEEE Trans. Neural Syst. Rehabil. Eng.*, vol. 26, no. 3, pp. 594–601, Feb. 2018.

[19] S. Gharehbaghi *et al.*, "Acoustic emissions from loaded and unloaded knees to assess joint health in patients with juvenile idiopathic arthritis," *IEEE J. Biomed. Health Inform.*, vol. 25, no. 9, pp. 3618–3626, Sep. 2021, doi: 10.1109/JBHI.2021.3081429.

[20] K. L. Scherpereel *et al.*, "Estimating knee joint load using acoustic emissions during ambulation," *Ann. Biomed. Eng.*, vol. 49, no. 3, pp. 1000–1011, 2021.

[21] K. Ch. Wierzcholski, "Friction forces for human hip joint lubrication at a naturally permeable cartilage," *Appl. Mechanics Eng.*, vol. 11, no. 3, 2006, Art. no. 515.

[22] D. Dowson, "Bio-tribology," *Faraday Discuss.*, vol. 156, no. 1, pp. 9–30, 2012.

[23] Z. M. Jin *et al.*, "(v) Biotribology," *Curr. Orthopaedics*, vol. 20, no. 1, pp. 32–40, 2006.

[24] Z. R. Zhoua and Z. M. Jin, "Biotribology: Recent progresses and future perspectives," *Biosurface Biotribology*, vol. 1, no. 1, pp. 3–24, 2015.

[25] Y. Wang and Q. J. Wang, *Stribeck Curves*. Boston, MA, USA: Springer, 2013, pp. 3365–3370.

[26] M. D. Hersey, "The laws of lubrication of horizontal journal bearings," *J. Washington Acad. Sci.*, vol. 4, no. 19, pp. 542–552, 1914.

[27] E. D. Bonnevie *et al.*, "Elastoviscous transitions of articular cartilage reveal a mechanism of synergy between lubricin and hyaluronic acid," *PloS One*, vol. 10, no. 11, 2015, Art. no. e0143415.

[28] C. H. Barnett, "Measurement and interpretation of synovial fluid viscosities," *Ann. Rheumatic Dis.*, vol. 17, no. 2, 1958, Art. no. 229.

[29] D. D. D'Lima *et al.*, "Knee joint forces: Prediction, measurement, and significance," in *Proc. Inst. Mech. Engineers, Part H: J. Eng. Med.*, 2012, vol. 226, no. 2, pp. 95–102.

[30] L. D. Duffell *et al.*, "Comparison of kinematic and kinetic parameters calculated using a cluster-based model and Vicon's plug-in gait," in *Proc. Inst. Mech. Engineers, Part H: J. Eng. Med.*, 2014, vol. 228, no. 2, pp. 206–210.

[31] G. K. Lenton *et al.*, "Tibiofemoral joint contact forces increase with load magnitude and walking speed but remain almost unchanged with different types of carried load," *PloS One*, vol. 13, no. 11, 2018, Art. no. e0206859.

[32] L. K. Shark *et al.*, "Knee acoustic emission: A potential biomarker for quantitative assessment of joint ageing and degeneration," *Med. Eng. Phys.*, vol. 33, no. 5, pp. 534–545, 2011.
[33] A. Mantoan *et al.*, "MOtoNMS: A MATLAB toolbox to process motion data for neuromusculoskeletal modeling and simulation," *Source Code Biol. Med.*, vol. 10, no. 1, pp. 1–14, 2015.
[34] S. L. Delp *et al.*, "OpenSim: Open-source software to create and analyze dynamic simulations of movement," *IEEE Trans. Biomed. Eng.*, vol. 54, no. 11, pp. 1940–1950, Nov. 2007.
[35] A. Seth *et al.*, "OpenSim: Simulating musculoskeletal dynamics and neuromuscular control to study human and animal movement," *PLoS Comput. Biol.*, vol. 14, no. 7, 2018, Art. no. e1006223.
[36] D. S. Catelli *et al.*, "A musculoskeletal model customized for squatting task," *Comput. Methods Biomech. Biomed. Eng.*, vol. 22, no. 1, pp. 21–24, 2019.
[37] C. Pizzolato *et al.*, "CEINMS: A toolbox to investigate the influence of different neural control solutions on the prediction of muscle excitation and joint moments during dynamic motor tasks," *J. Biomech.*, vol. 48, no. 14, pp. 3929–3936, 2015.
[38] E. Y. Hamid *et al.*, "Wavelet-based data compression of power system disturbances using the minimum description length criterion," *IEEE Trans. Power Del.*, vol. 17, no. 2, pp. 460–466, Apr. 2002.
[39] B. Semiz *et al.*, "Using knee acoustical emissions for sensing joint health in patients with Juvenile idiopathic arthritis: A pilot study," *IEEE Sensors J.*, vol. 18, no. 22, pp. 9128–9136, Nov. 2018.
[40] X. Valero and F. Alias, "Gammatone cepstral coefficients: Biologically inspired features for non-speech audio classification," *IEEE Trans. Multimedia*, vol. 14, pp. 1684–1689, 2012.
[41] T. Giannakopoulos and A. Pikrakis, *Introduction to Audio Analysis: A MATLAB Approach*. New York, NY, USA: Academic Press, 2014, pp. 59–106.
[42] P. A. Swinton *et al.*, "A biomechanical comparison of the traditional squat, powerlifting squat, and box squat," *J. Strength Conditioning Res.*, vol. 26, no. 7, pp. 1805–1816, 2012.
[43] R. A. Ibrahim, "Friction-induced vibration, chatter, squeal, and chaos-Part I: Mechanics of contact and friction," *Appl. Mech. Rev.*, pp. 209–226, 1994.
[44] G. D. Jay and K. A. Waller, "The biology of lubricin: Near frictionless joint motion," *Matrix Biol.*, vol. 39, pp. 17–24, 2014.
[45] R. M. Rangayyan, *Biomedical Signal Analysis*. Hoboken, NJ, USA: Wiley, 2015, pp. 393–396.
[46] A. Madkhali *et al.*, "Osteoarthritic synovial fluid rheology and correlations with protein concentration," *Biorheology*, vol. 53, no. 3-4, pp. 111–122, 2016.
[47] A. L. Kinney *et al.*, "Update on grand challenge competition to predict in vivo knee loads," *J. Biomechanical Eng.*, vol. 135, no. 2, pp. 1–4, 2013.